Code Review

What most likely happens

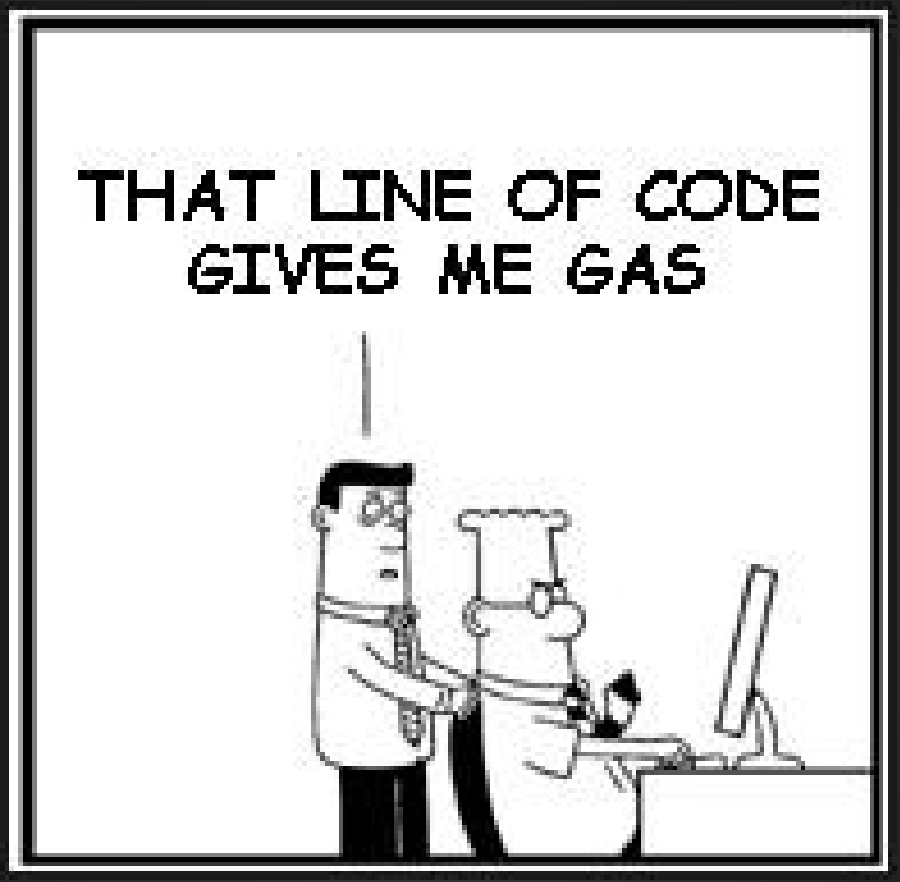

991 lines of code
5597 words
37448 characters (without blanks)

} 26 pages

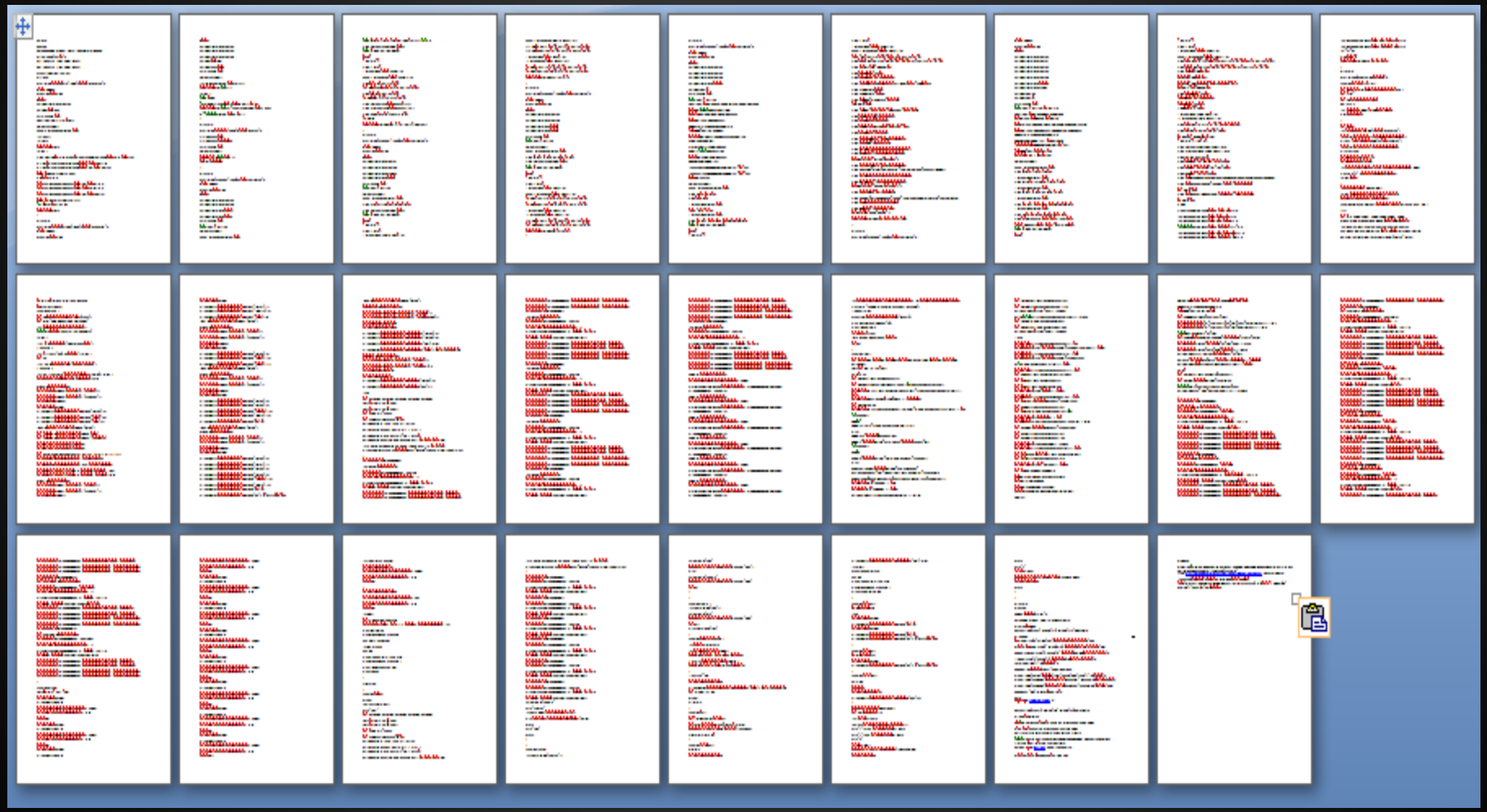

After abstracting the Javascript

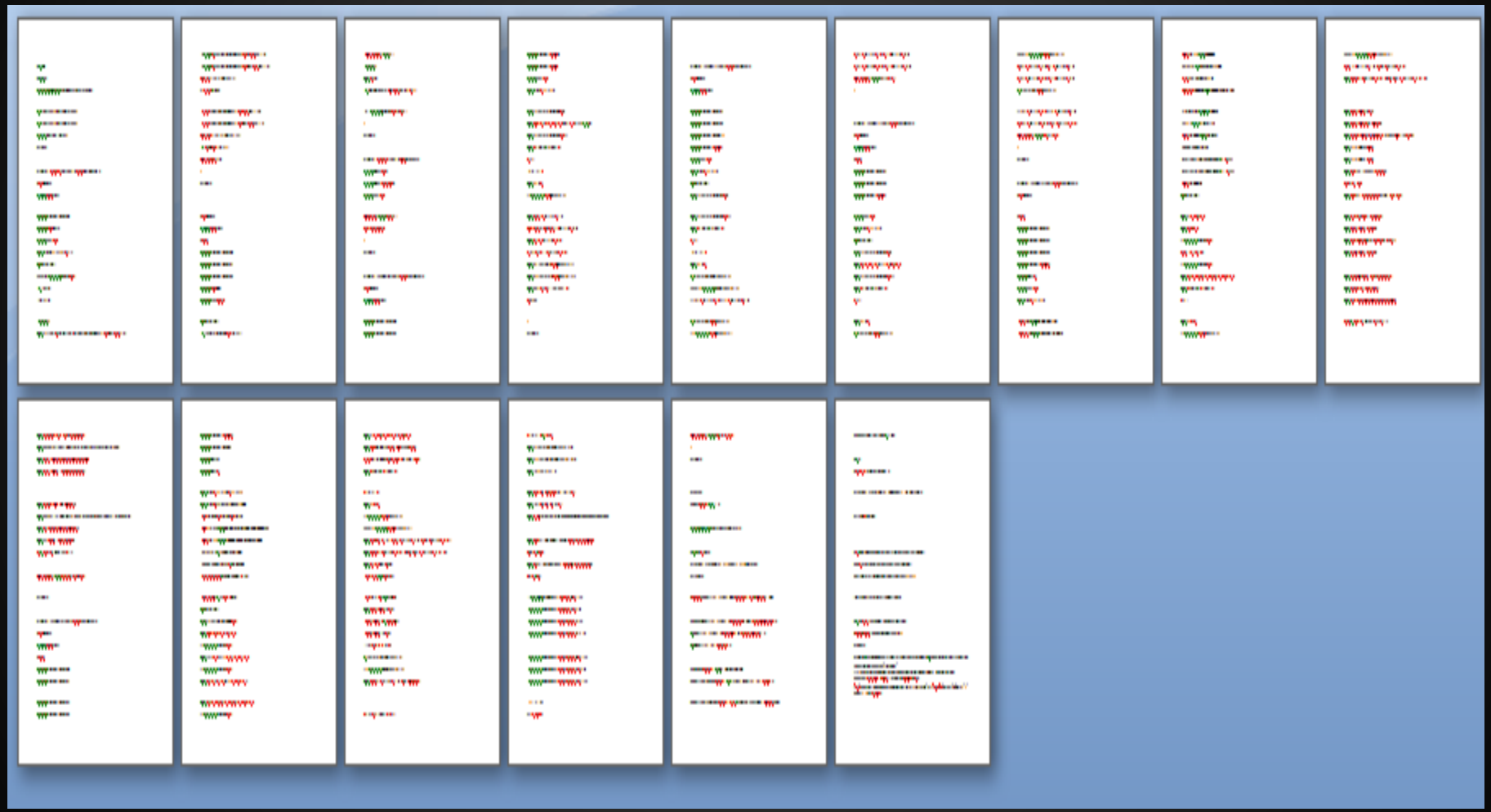

And then after abstracting the Webgl / shader

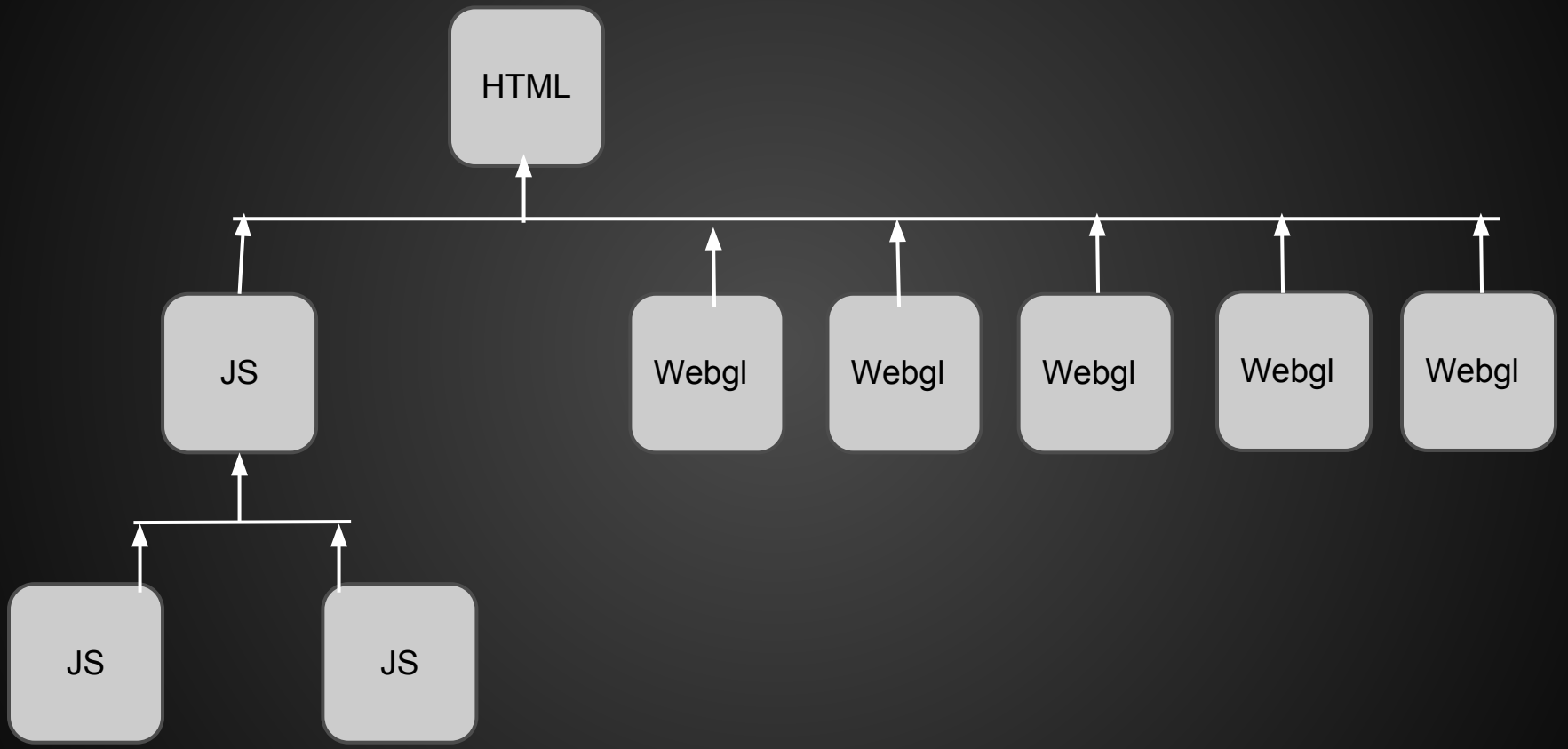
HTML
JS
Webgl
Webgl
Webgl
Webgl
Webgl
JS
JS

Why Webgl / Why Shader ?

Code of this type runs on a GPU:

- Allowing the CPU to do other work.
- GPU's are optimized to handle high level calculations.
  - Fast, Faster, Fastest !!!!!
    - Parallel

Code that is able to handle data points and calculations in parallel within a good amount of speed ... within the BROWSER !

- Project/environment setup time is less
- Able to run almost everywhere (internet is a plus)

Why in parallel ?

Lets get some background info .....

Loops (i.e. for, while, do,etc)

What are loops ?

In Biology

A form of cellular mitosis

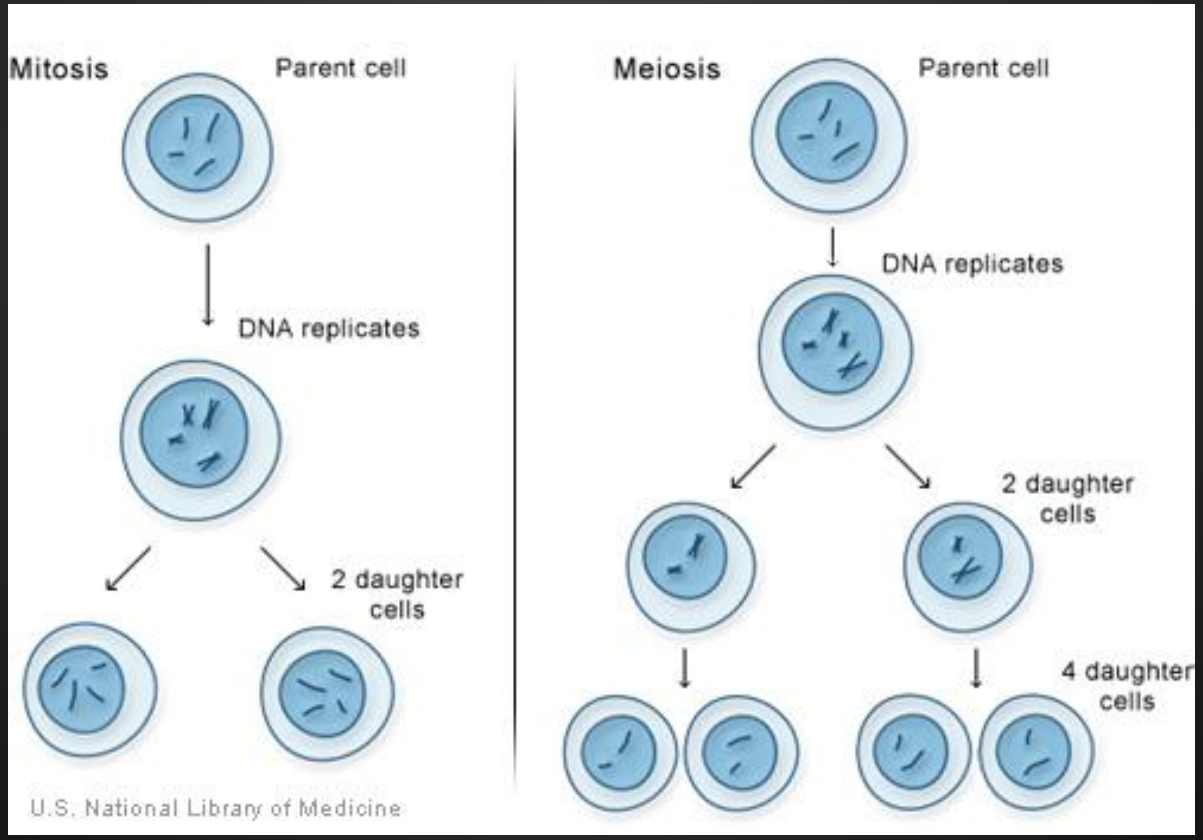

In mathematics

Iteration

$$
\begin{aligned}
u_0(t) &= 1, \\
u_1(t) &= 1 + bt, \\
u_2(t) &= 1 + bt + \frac{1}{2}b^2t^2 + \frac{ab}{\Gamma(3-\alpha)}t^{2-\alpha}, \\
u_3(t) &= 1 + bt + \frac{1}{2}b^2t^2 + \frac{ab}{\Gamma(3-\alpha)}t^{2-\alpha} + \frac{b^3}{6}t^3 + \frac{2ab^2}{\Gamma(4-\alpha)}t^{3-\alpha} + \frac{a^2b}{\Gamma(4-2\alpha)}t^{3-2\alpha}, \\
&\vdots
\end{aligned}
$$

What we want to see

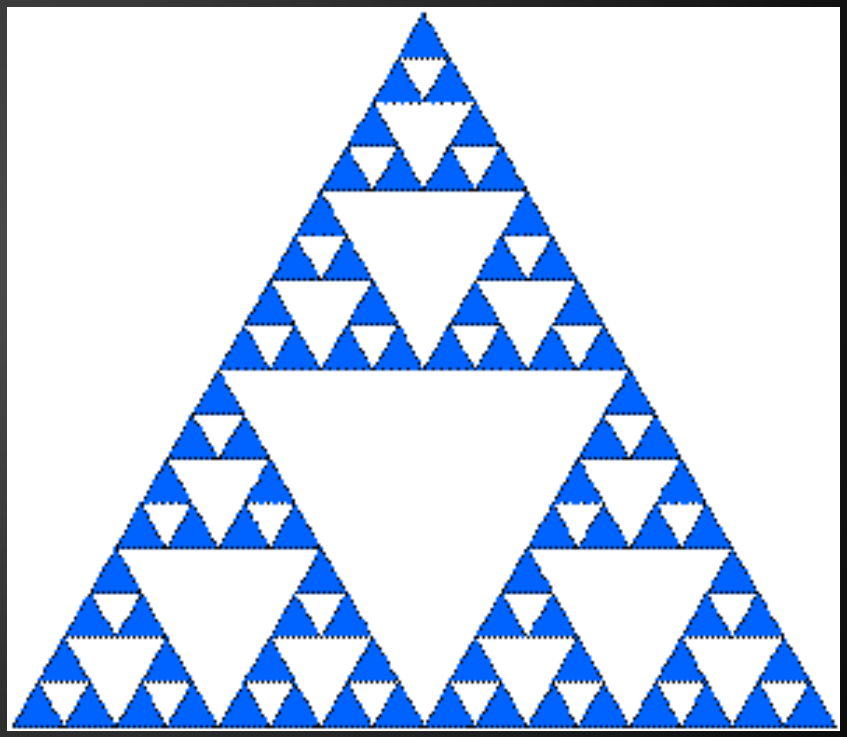

	Iteration	Number of Triangles Removed	Area of Each Triangle Removed
	1	$3^0 = 1$	$\frac{1}{4}$
	2	$3^1 = 3$	$\frac{1}{4}\left(\frac{1}{4}\right) = \frac{1}{4^2}$
	3	$3^2 = 9$	$\frac{1}{4^2}\left(\frac{1}{4}\right) = \frac{1}{4^3}$
	4	$3^3 = 27$	$\frac{1}{4^3}\left(\frac{1}{4}\right) = \frac{1}{4^4}$
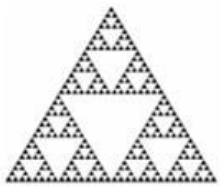	5	$3^4 = 81$	$\frac{1}{4^4}\left(\frac{1}{4}\right) = \frac{1}{4^5}$

Proof !!!

$$u_0(x,t) = 0,$$

$$u_1(x,t) = x\left(t + \frac{t^3}{3}\right),$$

$$u_2(x,t) = x\left(2t + \frac{t^3}{3} - 2t^{\cdots}\right.$$

$$u_3(x,t) = x\left(\frac{\cdots}{\cdots}\right.$$

$$\left. \frac{48t^{\cdots}}{\cdots} - \frac{34t^{11}}{51,975} - \frac{4t^{\cdots}}{12,285} - \frac{\cdots}{\cdots}\right)$$

$$\left. \frac{4}{\cdots\Gamma(3-\alpha)} - \cdots \left(\frac{1}{\Gamma(6-2\alpha)} - \frac{(5-\cdots}{\cdots}\right)\right)$$

$$\left. \frac{1}{\cdots\Gamma(3-\alpha)} + \frac{(6-\alpha)\Gamma(\cdots}{\cdots} \right)$$

$$+ \left(\frac{2}{\cdots\Gamma(5-\alpha)} - \frac{15(8-\cdots}{\cdots} \right)$$

$$- \left(\frac{63(10-\alpha)\Gamma(\cdots}{\cdots} \right)$$

$$- \frac{2t^{12-\alpha}}{63(12-\alpha)\Gamma(5-\alpha)} - \frac{t^{\cdots}}{(9-2\alpha)\Gamma(5-\alpha)^2} \Bigg),$$

$$\vdots$$

$$\frac{3t^{2-\alpha}}{\cdots - \alpha)}$$

$$\left. \cdots - \alpha)^2} \right) t^{3-2\alpha}$$

$$\frac{2t^{3-2\alpha}}{\cdots - 2\alpha)\Gamma(3-\alpha)\Gamma(5-\alpha)}$$

$$\frac{t^{3-2\alpha}}{\Gamma(4-2\alpha)}$$

In Physics

A form of boringness

boringness = insanity - (a varying of results which are expected)

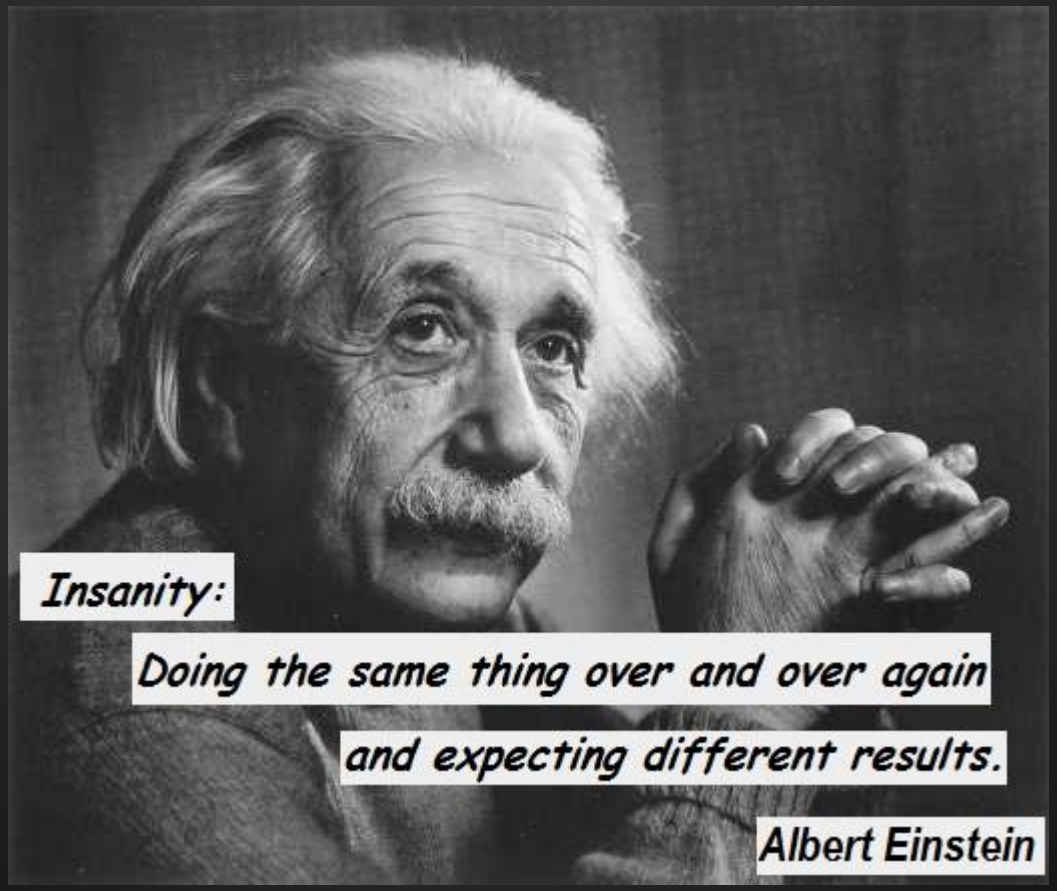

Okay okay, back to the parallel topic

Why do we want to do things in parallel ?

By breaking down sequential algorithms into smaller calculations, that have little to no dependences on each other, you allow them to become parallel algorithm(s).

Once the algorithm is in parallel form, the calculations can be optimized by removing it from a loop (i.e. sequential processing) and introducing parallelism.

What do we gain by doing this ?
Efficiency , which to a computer scientist means a speedup !

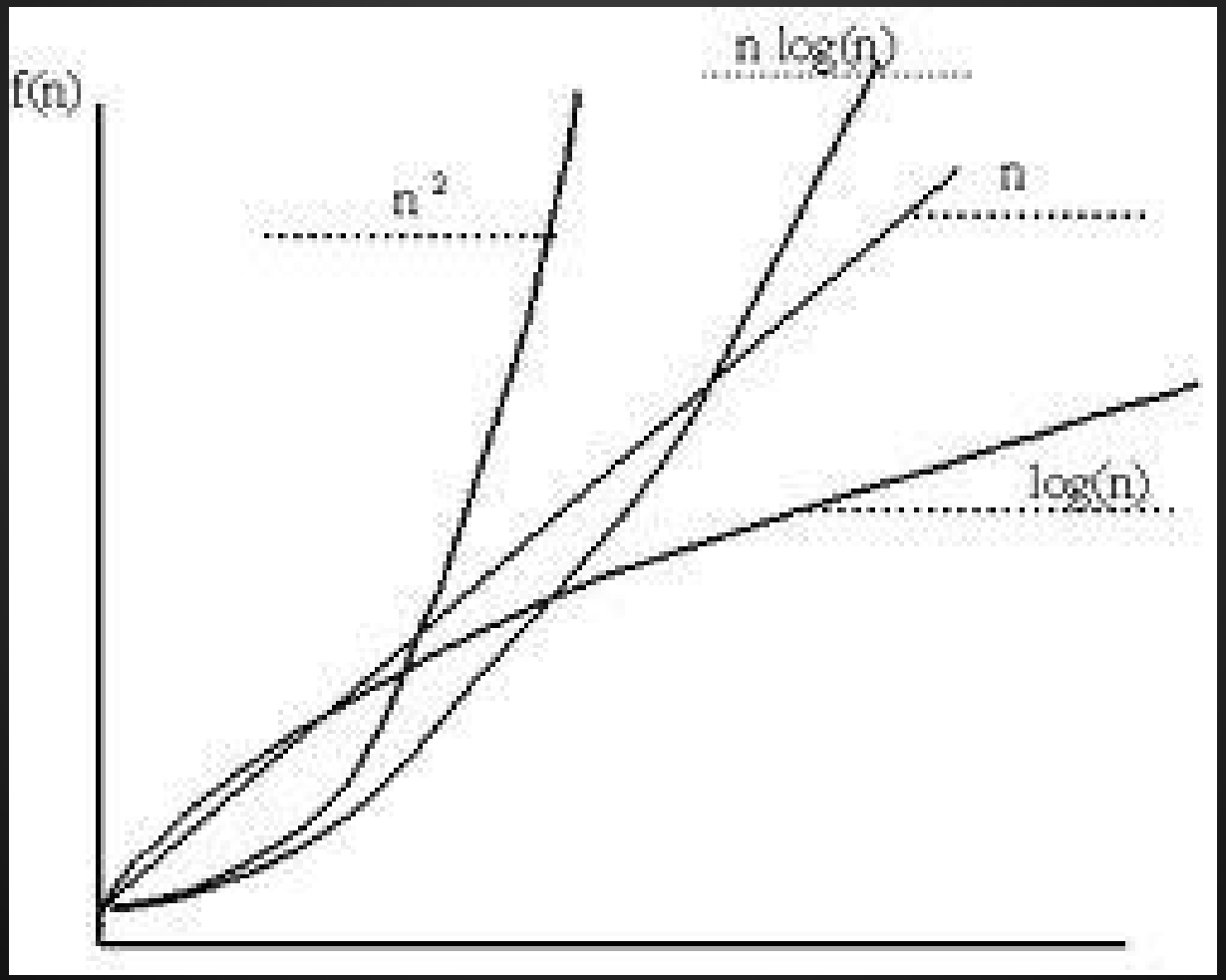

What does this represent ?

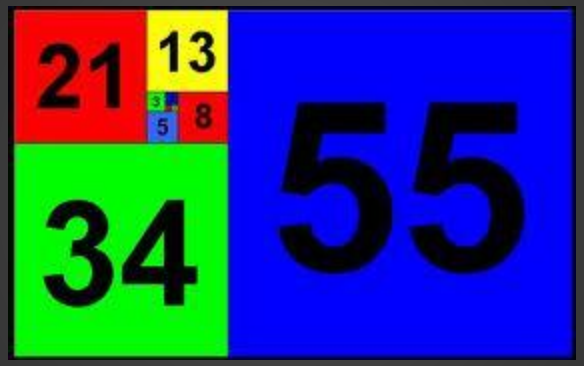

Hint

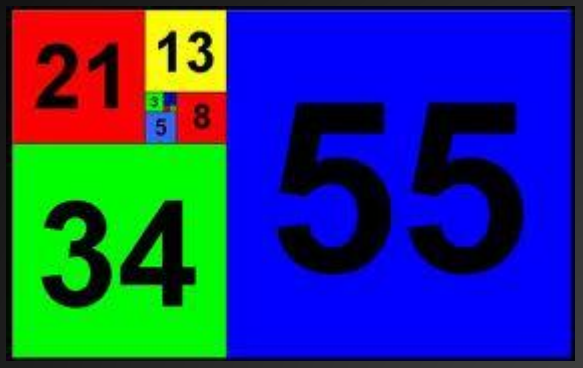

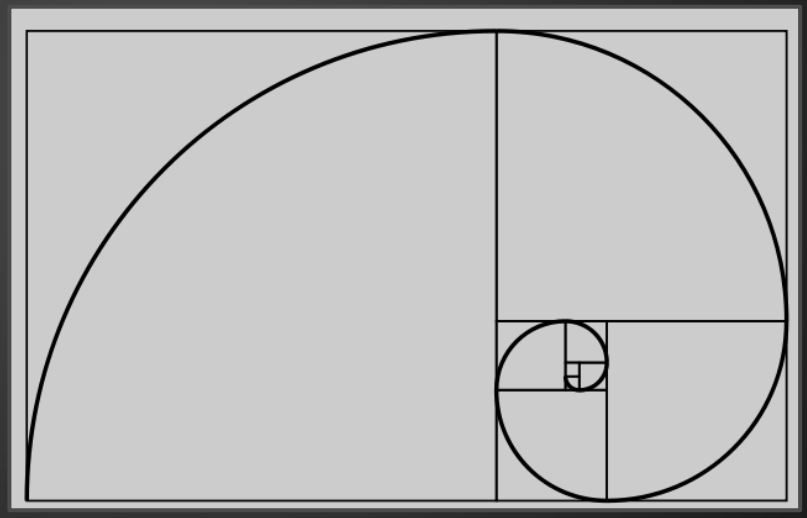

This is important because it has a pattern

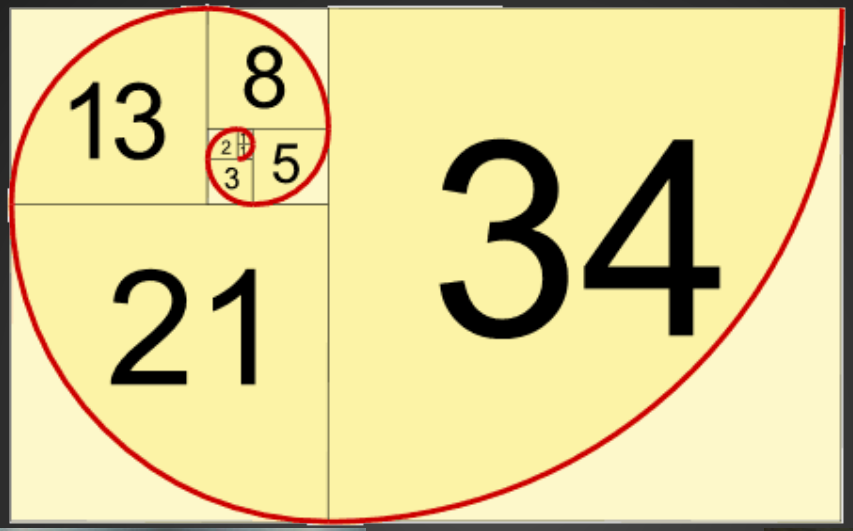

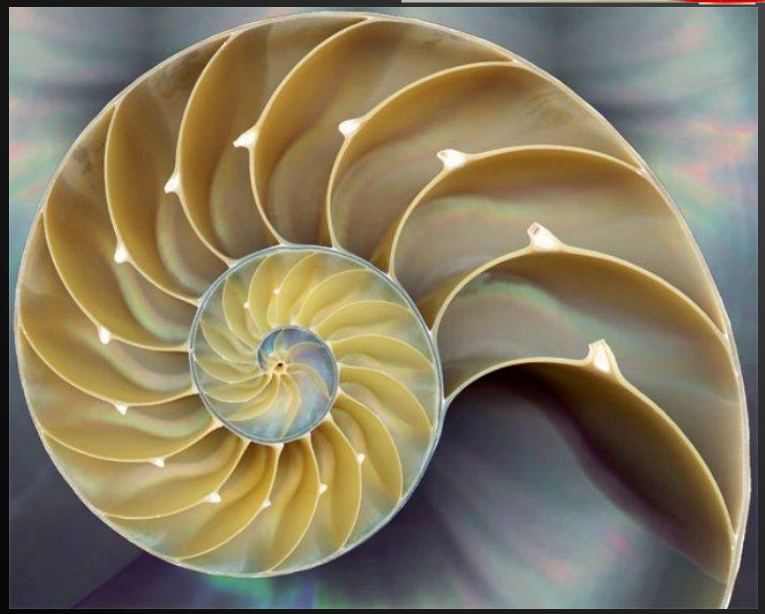

$$F(n) := \begin{cases} 0 & \text{if } n = 0; \\ 1 & \text{if } n = 1; \\ F(n-1) + F(n-2) & \text{if } n > 1. \end{cases}$$

```
public int Fibonacci(int n)
{
  if (n < 2)
    return n;
  else
    return Fibonacci(n - 1) + Fibonacci(n - 2);
}
```

Patterns

Can exist within

Numbers & Geometrics

How about with a procedure ? As in a procedural pattern:

a particular way of accomplishing something or of acting

a series of steps followed in a regular definite order

Euler's Method

$$y_{n+1} = y_n + h \cdot f(t_n, y_n)$$

Lets try one:

Use Euler's method with step size x =.1 to estimate y(.5) where y(x) is the solution of the initial value problem, y(0)=3,
$y' = f(x_n, y_n) = 3x^2(2-y)$.

x	y	$3x^2(2-y)$	$y_n = y_{n-1} + \Delta x \cdot f'(x_{n-1}, y_{n-1})$

x	y	$3x^2(2-y)$	$y_n = y_{n-1} + \Delta x \cdot f'(x_{n-1}, y_{n-1})$
0	3	0	3
0.1	3	−0.03	2.997
0.2	2.997	−0.11964	2.985036
0.3	2.985036	−0.265959	2.9584400
0.4	2.958440	−0.460051	2.912434
0.5	2.912434	−0.684326	2.844002
0.6	2.844002	−0.911522	2.752850
0.7	2.752850	−1.106689	2.642181
0.8	2.642181	−1.232987	2.518882
0.9	2.518882	−1.260884	2.392793
1	2.392793		

$y(1) \approx 2.393$

Should we make a procedure like this parallel or sequential ?

Lets try to implement Euler's Method ...

Some code ...

```
public void init()
{


  // Variables
  double t, y, vy;
  double total_t;
  int n;

  // Constants
  double y0 =  0.0;
  double v0 =  0.0;
  double g  = -9.80;// meter per sec**2

  // Version 1
  double dt =  0.1;
  int n_steps = 10;
  y = y0;
  vy = v0;

  for( n=0; n< n_steps; n++)
  {
    y = y + vy * dt;
    vy = vy + g * dt;
  }

  total_t = n * dt;

  System.out.println("Version 1, dt=0.1 ");
  System.out.println("Time = " + total_t);
  System.out.println("y = " + y +", vy = " + vy);
  System.out.println();
```

Just an example

Going Deeper

We now want to get deeper into the code.
We are going to download exercises.

Look for patterns in the code that will optimize it as well as readability.

(Remember abstraction can be your friend)

CLB.CharlesB@gmail.com

Before

```
299 function draw(){
300
301   for(var i = 0; i < nit; i++){
302     gl.useProgram(prog0);
303     gl.uniform1i(loc0, 4);
304     gl.bindFramebuffer(gl.FRAMEBUFFER, FBO0);
305     gl.drawArrays(gl.TRIANGLE_STRIP, 0, 4);
306     gl.flush();
307     gl.useProgram(prog1);
308     gl.uniform1i(loc1, 4);
309     gl.bindFramebuffer(gl.FRAMEBUFFER, FBO1);
310     gl.drawArrays(gl.TRIANGLE_STRIP, 0, 4);
311     gl.flush();
312     gl.useProgram(prog2);
313     gl.uniform1i(loc2, 4);
314     gl.bindFramebuffer(gl.FRAMEBUFFER, FBO2);
315     gl.drawArrays(gl.TRIANGLE_STRIP, 0, 4);
316     gl.flush();
317     gl.useProgram(prog3);
318     gl.uniform1i(loc3, 4);
319     gl.bindFramebuffer(gl.FRAMEBUFFER, FBO3);
320     gl.drawArrays(gl.TRIANGLE_STRIP, 0, 4);
321     gl.flush();
322     gl.useProgram(prog4);
323     gl.uniform1i(loc4, 4);
324     gl.bindFramebuffer(gl.FRAMEBUFFER, FBO5);
325     gl.drawArrays(gl.TRIANGLE_STRIP, 0, 4);
326     gl.flush();
327
328     gl.useProgram(prog0);
329     gl.uniform1i(loc0, 5);
330     gl.bindFramebuffer(gl.FRAMEBUFFER, FBO0);
331     gl.drawArrays(gl.TRIANGLE_STRIP, 0, 4);
332     gl.flush();
333     gl.useProgram(prog1);
334     gl.uniform1i(loc1, 5);
```

After

```
299 function draw(){
300     var setLength = 5;
301     var progSet = [prog0,prog1,prog2,prog3,prog4];
302     var locSet  = [loc0,loc1,loc2,loc3,loc4];
303     var FBOSet  = [FBO0,FBO1,FBO2,FBO3,FBO4,FBO5];
304   for(var i = 0; i < nit; i++){
305 
306     for(var innerIndex=0; innerIndex< setLength; innerIndex++){
307         gl.useProgram(progSet[innerIndex]);
308         gl.uniform1i(locSet[innerIndex], 4);
309         if(innerIndex==4){
310             gl.bindFramebuffer(gl.FRAMEBUFFER, FBOSet[innerIndex+1]);
311         }else{
312             gl.bindFramebuffer(gl.FRAMEBUFFER, FBOSet[innerIndex]);
313         }
314         gl.drawArrays(gl.TRIANGLE_STRIP, 0, 4);
315         gl.flush();
316     }
317 
318 /*
319     gl.useProgram(prog4);
320     gl.uniform1i(loc4, 4);
321     gl.bindFramebuffer(gl.FRAMEBUFFER, FBO5);
322     gl.drawArrays(gl.TRIANGLE_STRIP, 0, 4);
323     gl.flush();
324 */
325 
326     for(var innerIndex=0; innerIndex< setLength; innerIndex++){
327         gl.useProgram(progSet[innerIndex]);
328         gl.uniform1i(locSet[innerIndex], 5);
329         gl.bindFramebuffer(gl.FRAMEBUFFER, FBOSet[innerIndex]);
330         gl.drawArrays(gl.TRIANGLE_STRIP, 0, 4);
331         gl.flush();
332     }
333 
```

Why is this important ?
Because now you have a better understanding and working knowledge of:

Iteration within code
Being able to follow a procedure within a loop
Recognizing patterns within code
Converting procedures into code (even if already coded)

Is the code we just modified optimized, readable, or both ?

Going Further

Now that we all have the skills we need, lets look at the paper(s), it's algorithms, and the code .....

Am J Physiol Heart Circ Physiol 286: H1573–H1589, 2004.
First published December 4, 2003; 10.1152/ajpheart.00794.2003.

A model for human ventricular tissue

K. H. W. J. ten Tusscher,[1] D. Noble,[2] P. J. Noble,[2] and A. V. Panfilov[1,3]

[1]*Department of Theoretical Biology, Utrecht University, 3584 CH Utrecht, The Netherlands; and* [2]*University Laboratory of Physiology, University of Oxford, Oxford OX1 3PT; and* [3]*Division of Mathematics, University of Dundee, Dundee DD1 4HN, United Kingdom*

Submitted 9 August 2003; accepted in final form 2 December 2003

Ten Tusscher, K. H. W. J., D. Noble, P. J. Noble, and A. V. Panfilov. A model for human ventricular tissue. *Am J Physiol Heart Circ Physiol* 286: H1573–H1589, 2004. First published December 4, 2003; 10.1152/ajpheart.00794.2003.—The experimental and clinical possibilities for studying cardiac arrhythmias in human ventricular myocardium are very limited. Therefore, the use of alternative methods such as computer simulations is of great importance. In this article we introduce a mathematical model of the action potential of human ventricular cells that, while including a high level of electrophysio-

constrained to surface recordings. Computer simulations of arrhythmias in the human heart can overcome some of these problems.

To perform simulation studies of reentrant arrhythmias in human ventricles we need a mathematical model that on the one hand reproduces detailed properties of single human ventricular cells, such as the major ionic currents, calcium transients, and AP duration (APD) restitution (APDR), and impor-

Let's open the paper "A Model For Human Ventricular Tissue"

MATERIALS AND METHODS

General

The cell membrane is modeled as a capacitor connected in parallel with variable resistances and batteries representing the different ionic currents and pumps. The electrophysiological behavior of a single cell can hence be described with the following differential equation (23)

$$\frac{dV}{dt} = -\frac{I_{ion} + I_{stim}}{C_m} \quad (1)$$

where V is voltage, t is time, I_{ion} is the sum of all transmembrane ionic currents, I_{stim} is the externally applied stimulus current, and C_m is cell capacitance per unit surface area.

Similarly, ignoring the discrete character of microscopic cardiac cell structure, a 2D sheet of cardiac cells can be modeled as a continuous system with the following partial differential equation (23)

$$\frac{\partial V}{\partial t} = -\frac{I_{ion} + I_{stim}}{C_m} + \frac{1}{\rho_x S_x C_m}\frac{\partial^2 V}{\partial x^2} + \frac{1}{\rho_y S_y C_m}\frac{\partial^2 V}{\partial y^2} \quad (2)$$

where ρ_x and ρ_y are the cellular resistivity in the x and y directions, S_x and S_y are the surface-to-volume ratio in the x and y directions, and I_{ion} is the sum of all transmembrane ionic currents given by the following equation

$$I_{ion} = I_{Na} + I_{K1} + I_{to} + I_{Kr} + I_{Ks} + I_{CaL} + I_{NaCa} + I_{NaK} + I_{pCa} + I_{pK} + I_{bCa} + I_{bNa} \quad (3)$$

where I_{NaCa} is Na^+/Ca^{2+} exchanger current, I_{NaK} is Na^+/K^+ pump current, I_{pCa} and I_{pK} are plateau Ca^{2+} and K^+ currents, and I_{bCa} and I_{bK} are background Ca^{2+} and K^+ currents.

V_{SR}	Sarcoplasmic reticulum volume	1,094 μm^3
K_O	Extracellular K^+ concentration	5.4 mM
Na_O	Extracellular Na^+ concentration	140 mM
Ca_O	Extracellular Ca^{2+} concentration	2 mM
G_{Na}	Maximal I_{Na} conductance	14.838 nS/pF
G_{K1}	Maximal I_{K1} conductance	5.405 nS/pF
G_{to}, epi, M	Maximal epicardial I_{to} conductance	0.294 nS/pF
G_{to}, endo	Maximal endocardial I_{to} conductance	0.073 nS/pF
G_{Kr}	Maximal I_{Kr} conductance	0.096 nS/pF
G_{Ks}, epi, endo	Maximal epi- and endocardial I_{Ks} conductance	0.245 nS/pF
G_{Ks}, M	Maximal M cell I_{Ks} conductance	0.062 nS/pF
p_{KNa}	Relative I_{Ks} permeability to Na^+	0.03
G_{CaL}	Maximal I_{CaL} conductance	1.75^{-4} $cm^3 \cdot \mu F^{-1} \cdot s^{-1}$
k_{NaCa}	Maximal I_{NaCa}	1,000 pA/pF
γ	Voltage dependence parameter of I_{NaCa}	0.35
K_{mCa}	Ca_i half-saturation constant for I_{NaCa}	1.38 mM
K_{mNai}	Na_i half-saturation constant for I_{NaCa}	87.5 mM
k_{sat}	Saturation factor for I_{NaCa}	0.1
α	Factor enhancing outward nature of I_{NaCa}	2.5
P_{NaK}	Maximal I_{NaK}	1.362 pA/pF
K_{mK}	K_O half-saturation constant of I_{NaK}	1 mM
K_{mNa}	Na_i half-saturation constant of I_{NaK}	40 mM
G_{pk}	Maximal I_{pK} conductance	0.0146 nS/pF
G_{pCa}	Maximal I_{pCa} conductance	0.025 nS/pF
K_{pCa}	Ca_i half-saturation constant of I_{pCa}	0.0005 mM
G_{bNa}	Maximal I_{bNa} conductance	0.00029 nS/pF
G_{bCa}	Maximal I_{bCa} conductance	0.000592 nS/pF
V_{maxup}	Maximal I_{up}	0.000425 mM/ms
K_{up}	Half-saturation constant of I_{up}	0.00025 mM
a_{rel}	Maximal Ca_{SR}-dependent I_{rel}	16.464 mM/s
b_{rel}	Ca_{SR} half-saturation constant of I_{rel}	0.25 mM
c_{rel}	Maximal Ca_{SR}-independent I_{rel}	8.232 mM/s
V_{leak}	Maximal I_{leak}	0.00008 ms^{-1}
Buf_c	Total cytoplasmic buffer concentration	0.15 mM

Under Materials And Methods
on page 2 (in PDF form)

Table 1. *Model parameters*

Parameter	Definition	Value
R	Gas constant	8.3143 J·K^{-1}·mol^{-1}
T	Temperature	310 K
F	Faraday constant	96.4867 C/mmol
C_m	Cell capacitance per unit surface area	2 μF/cm^2
S	Surface-to-volume ratio	0.2 μm^{-1}
ρ	Cellular resistivity	162 Ω·cm
V_C	Cytoplasmic volume	16,404 μm^3
V_{SR}	Sarcoplasmic reticulum volume	1,094 μm^3
K_O	Extracellular K^+ concentration	5.4 mM
Na_O	Extracellular Na^+ concentration	140 mM
Ca_O	Extracellular Ca^{2+} concentration	2 mM
G_{Na}	Maximal I_{Na} conductance	14.838 nS/pF
G_{K1}	Maximal I_{K1} conductance	5.405 nS/pF
G_{to}, epi, M	Maximal epicardial I_{to} conductance	0.294 nS/pF
G_{to}, endo	Maximal endocardial I_{to} conductance	0.073 nS/pF
G_{Kr}	Maximal I_{Kr} conductance	0.096 nS/pF
G_{Ks}, epi, endo	Maximal epi- and endocardial I_{Ks} conductance	0.245 nS/pF
G_{Ks}, M	Maximal M cell I_{Ks} conductance	0.062 nS/pF
p_{KNa}	Relative I_{Ks} permeability to Na^+	0.03
G_{CaL}	Maximal I_{CaL} conductance	1.75^{-4} cm^3·μF^{-1}·s^{-1}
k_{NaCa}	Maximal I_{NaCa}	1,000 pA/pF
γ	Voltage dependence parameter of I_{NaCa}	0.35
K_{mCa}	Ca_i half-saturation constant for I_{NaCa}	1.38 mM
K_{mNai}	Na_i half-saturation constant for I_{NaCa}	87.5 mM
k_{sat}	Saturation factor for I_{NaCa}	0.1
α	Factor enhancing outward nature of I_{NaCa}	2.5
P_{NaK}	Maximal I_{NaK}	1.362 pA/pF
K_{mK}	K_O half-saturation constant of I_{NaK}	1 mM
K_{mNa}	Na_i half-saturation constant of I_{NaK}	40 mM
G_{pk}	Maximal I_{pK} conductance	0.0146 nS/pF
G_{pCa}	Maximal I_{pCa} conductance	0.025 nS/pF
K_{pCa}	Ca_i half-saturation constant of I_{pCa}	0.0005 mM
G_{bNa}	Maximal I_{bNa} conductance	0.00029 nS/pF
G_{bCa}	Maximal I_{bCa} conductance	0.000592 nS/pF
V_{maxup}	Maximal I_{up}	0.000425 mM/ms
K_{up}	Half-saturation constant of I_{up}	0.00025 mM
a_{rel}	Maximal Ca_{SR}-dependent I_{rel}	16.464 mM/s
b_{rel}	Ca_{SR} half-saturation constant of I_{rel}	0.25 mM
c_{rel}	Maximal Ca_{SR}-independent I_{rel}	8.232 mM/s
V_{leak}	Maximal I_{leak}	0.00008 ms^{-1}
Buf_c	Total cytoplasmic buffer concentration	0.15 mM
K_{bufc}	Ca_i half-saturation constant for cytoplasmic buffer	0.001 mM
Buf_{sr}	Total sarcoplasmic buffer concentration	10 mM
K_{bufsr}	Ca_{SR} half-saturation constant for sarcoplasmic buffer	0.3 mM

where ρ_x and ρ_y are the cellular resistivity in the x and y directions, S_x and S_y are the surface-to-volume ratio in the x and y directions, and I_{ion} is the sum of all transmembrane ionic currents given by the following equation

$$I_{ion} = I_{Na} + I_{K1} + I_{to} + I_{Kr} + I_{Ks} + I_{CaL} + I_{NaCa} + I_{NaK} + I_{pCa} + I_{pK} + I_{bCa} + I_{bNa} \quad (3)$$

where I_{NaCa} is Na^+/Ca^{2+} exchanger current, I_{NaK} is Na^+/K^+ pump current, I_{pCa} and I_{pK} are plateau Ca^{2+} and K^+ currents, and I_{bCa} and I_{bK} are background Ca^{2+} and K^+ currents.

Physical units used in our model are as follows: time (t) in milliseconds, voltage (V) in millivolts, current densities (I_X) in picoamperes per picofarad, conductances (G_X) in nanosiemens per picofarad, and intracellular and extracellular ionic concentrations (X_i, X_o) in millimoles per liter. The equations for the ionic currents are specified in *Membrane Currents*.

For one-dimensional (1D) computations cell capacitance per unit surface area is taken as $C_m = 2.0\ \mu F/cm^2$ and surface-to-volume ratio is set to $S = 0.2\ \mu m^{-1}$, following Bernus et al. (3). To obtain a maximum planar conduction velocity (CV) of 70 cm/s, the velocity found for conductance along the fiber direction in human myocardium by Taggart et al. (61), a cellular resistivity $\rho = 162\ \Omega cm$ was required. This is comparable to the $\rho = 180\ \Omega cm$ used by Bernus et al. (3) and the $\rho = 181\ \Omega cm$ used by Jongsma and Wilders (29), and it results in a "diffusion" coefficient $D = 1/(\rho S C_m)$ of 0.00154 cm^2/ms. Because in 2D we did not intend to study the effects of anisotropy, we use the same values for ρ_x and ρ_y and for S_x and S_y. Parameters of the model are given in Table 1.

For 1D and 2D computations, the forward Euler method was used to integrate *Eq. 1*. A space step of $\Delta x = 0.1$–0.2 mm and a time step of $\Delta t = 0.01$–0.02 ms were used. To integrate the Hodgkin-Huxley-

K_{mNa}	Na_i half-saturation constant of I_{NaK}	40 mM
G_{pk}	Maximal I_{pK} conductance	0.0146 nS/pF
G_{pCa}	Maximal I_{pCa} conductance	0.025 nS/pF
K_{pCa}	Ca_i half-saturation constant of I_{pCa}	0.0005 mM
G_{bNa}	Maximal I_{bNa} conductance	0.00029 nS/pF
G_{bCa}	Maximal I_{bCa} conductance	0.000592 nS/pF
V_{maxup}	Maximal I_{up}	0.000425 mM/ms
K_{up}	Half-saturation constant of I_{up}	0.00025 mM
a_{rel}	Maximal Ca_{SR}-dependent I_{rel}	16.464 mM/s
b_{rel}	Ca_{SR} half-saturation constant of I_{rel}	0.25 mM
c_{rel}	Maximal Ca_{SR}-independent I_{rel}	8.232 mM/s
V_{leak}	Maximal I_{leak}	0.00008 ms^{-1}
Buf_c	Total cytoplasmic buffer concentration	0.15 mM
K_{bufc}	Ca_i half-saturation constant for cytoplasmic buffer	0.001 mM
Buf_{sr}	Total sarcoplasmic buffer concentration	10 mM
K_{bufsr}	Ca_{SR} half-saturation constant for sarcoplasmic buffer	0.3 mM

We test the accuracy of our numerical simulations in a cable of cells by varying both the time and space steps of integration. The results of these tests are shown in Table 2. From Table 2 it follows that, with a $\Delta x = 0.2$ mm, decreasing Δt from 0.02 to 0.0025 ms leads to a 3.7% increase in CV. Similarly, with $\Delta t = 0.02$ ms, decreasing Δx from 0.2 to 0.1 mm leads to a an increase in CV of 4.6%. The changes in CV occurring for changes in space and time integration steps are similar to those occurring in other models (see, for example, Ref. 52). The time and space steps used in most computations are $\Delta t = 0.02$ ms and $\Delta x = 0.2$ mm, similar to values used in other studies (3, 6, 52, 69). Major conclusions of our model were tested for smaller space and time steps; the results were only slightly different.

We want to better under what makes up I_{ion}

where ρ_x and ρ_y are the cellular resistivity in the x and y directions, S_x and S_y are the surface-to-volume ratio in the x and y directions, and I_{ion} is the sum of all transmembrane ionic currents given by the following equation

$$I_{ion} = I_{Na} + I_{K1} + I_{to} + I_{Kr} + I_{Ks} + I_{CaL} + I_{NaCa} + I_{NaK} + I_{pCa} + I_{pK} + I_{bCa} + I_{bNa} \quad (3)$$

where I_{NaCa} is Na^+/Ca^{2+} exchanger current, I_{NaK} is Na^+/K^+ pump current, I_{pCa} and I_{pK} are plateau Ca^{2+} and K^+ currents, and I_{bCa} and I_{bK} are background Ca^{2+} and K^+ currents.

Physical units used in our model are as follows: time (t) in milliseconds, voltage (V) in millivolts, current densities (I_X) in picoamperes per picofarad, conductances (G_X) in nanosiemens per picofarad, and intracellular and extracellular ionic concentrations (X_i, X_o) in millimoles per liter. The equations for the ionic currents are specified in *Membrane Currents*.

For one-dimensional (1D) computations cell capacitance per unit surface area is taken as $C_m = 2.0\ \mu F/cm^2$ and surface-to-volume ratio is set to $S = 0.2\ \mu m^{-1}$, following Bernus et al. (3). To obtain a maximum planar conduction velocity (CV) of 70 cm/s, the velocity found for conductance along the fiber direction in human myocardium by Taggart et al. (61), a cellular resistivity $\rho = 162\ \Omega cm$ was required. This is comparable to the $\rho = 180\ \Omega cm$ used by Bernus et al. (3) and the $\rho = 181\ \Omega cm$ used by Jongsma and Wilders (29), and it results in a "diffusion" coefficient $D = 1/(\rho S C_m)$ of 0.00154 cm^2/ms. Because in 2D we did not intend to study the effects of anisotropy, we use the same values for ρ_x and ρ_y and for S_x and S_y. Parameters of the model are given in Table 1.

For 1D and 2D computations, the forward Euler method was used to integrate *Eq. 1*. A space step of $\Delta x = 0.1$–0.2 mm and a time step of $\Delta t = 0.01$–0.02 ms were used. To integrate the Hodgkin-Huxley-

K_{mNa}	Na_i half-saturation constant of I_{NaK}	40 mM
G_{pk}	Maximal I_{pK} conductance	0.0146 nS/pF
G_{pCa}	Maximal I_{pCa} conductance	0.025 nS/pF
K_{pCa}	Ca_i half-saturation constant of I_{pCa}	0.0005 mM
G_{bNa}	Maximal I_{bNa} conductance	0.00029 nS/pF
G_{bCa}	Maximal I_{bCa} conductance	0.000592 nS/pF
V_{maxup}	Maximal I_{up}	0.000425 mM/ms
K_{up}	Half-saturation constant of I_{up}	0.00025 mM
a_{rel}	Maximal Ca_{SR}-dependent I_{rel}	16.464 mM/s
b_{rel}	Ca_{SR} half-saturation constant of I_{rel}	0.25 mM
c_{rel}	Maximal Ca_{SR}-independent I_{rel}	8.232 mM/s
V_{leak}	Maximal I_{leak}	0.00008 ms^{-1}
Buf_c	Total cytoplasmic buffer concentration	0.15 mM
K_{bufc}	Ca_i half-saturation constant for cytoplasmic buffer	0.001 mM
Buf_{sr}	Total sarcoplasmic buffer concentration	10 mM
K_{bufsr}	Ca_{SR} half-saturation constant for sarcoplasmic buffer	0.3 mM

We test the accuracy of our numerical simulations in a cable of cells by varying both the time and space steps of integration. The results of these tests are shown in Table 2. From Table 2 it follows that, with a $\Delta x = 0.2$ mm, decreasing Δt from 0.02 to 0.0025 ms leads to a 3.7% increase in CV. Similarly, with $\Delta t = 0.02$ ms, decreasing Δx from 0.2 to 0.1 mm leads to a an increase in CV of 4.6%. The changes in CV occurring for changes in space and time integration steps are similar to those occurring in other models (see, for example, Ref. 52). The time and space steps used in most computations are $\Delta t = 0.02$ ms and $\Delta x = 0.2$ mm, similar to values used in other studies (3, 6, 52, 69). Major conclusions of our model were tested for smaller space and time steps; the results were only slightly different.

We want to better under what makes up I_{ion}

Table 2. *Numerical accuracy of conduction velocity for different Δt and Δx*

	Conduction Velocity, cm/s			
Δx, cm	Δt = 0.0025 ms	Δt = 0.005 ms	Δt = 0.01 ms	Δt = 0.02 ms
0.010	75.4	75.0	74.2	72.5
0.015	74.4	73.8	73.0	71.5
0.020	71.9	71.5	70.8	69.3
0.030	67.8	67.4	66.8	65.7
0.040	63.2	63.0	62.6	61.7

applied at a frequency of 1 Hz and a strength of two times the threshold value, followed by a S2 extrastimulus delivered at some diastolic interval (DI) after the AP generated by the last S1 stimulus. The APDR curve is generated by decreasing DI and plotting APD generated by the S2 stimulus against DI. The second restitution protocol is called the dynamic restitution protocol. It was first proposed by Koller et al. (32) as being a more relevant determinant of spiral wave stability than S1-S2 restitution. The protocol consists of a series of stimuli at a certain cycle length until a steady-state APD is reached; after that, cycle length is decreased. The APDR curve is obtained by plotting steady-state APDs against steady-state DIs. CV restitution (CVR) was simulated in a linear strand of 400 cells by pacing it at one end at various frequencies and measuring CV in the middle of the cable.

Spiral waves were initiated in 2D sheets of ventricular tissue with the S1-S2 protocol. We first applied a single S1 stimulus along the entire length of one side of the tissue, producing a planar wave front

Membrane Currents

Fast Na^+ current: I_{Na}. We use the three gates formulation of I_{Na} first introduced by Beeler and Reuter (1)

$$I_{Na} = G_{Na} m^3 h j (V - E_{Na}) \quad (4)$$

where m is an activation gate, h is a fast inactivation gate, and j is a slow inactivation gate. Each of these gates is governed by Hodgkin-Huxley-type equations for gating variables and characterized by a steady-state value and a time constant for reaching this steady-state value, both of which are functions of membrane potential (see APPENDIX).

The steady-state activation curve (m_∞^3) is fitted to data on steady-state activation of wild-type human Na^{2+} channels expressed in HEK-293 cells from Nagatomo et al. (44). Experimental data were extrapolated to 37°. Because there is no equivalent to the Q_{10} values used to extrapolate time constants to different temperatures, a linear extrapolation was used based on a comparison of values obtained at 23° and 33°. Note that similar Na^+ channel activation data were obtained by others (64, 40, 55). Figure 1*A* shows the steady-state activation curve used in our model. For comparison, temperature-corrected experimental data are added.

The steady-state curve for inactivation ($h_\infty \times j_\infty$) is fitted to steady-state inactivation data from Nagatomo et al. (44). Again, data were extrapolated to 37°. Similar inactivation data were obtained by others (55, 64). Figure 1*B* shows the steady-state inactivation curve used in our model together with temperature-corrected experimental data. Note that for resting membrane potentials the h and j gates are partially inactivated.

The time constants τ_h and τ_j are derived from current decay (typically, V greater than −50 mV) and current recovery experiments

Under Membrane Currents
on page 3 (in PDF form)

Alternans and spiral breakup in a human ventricular tissue model

K. H. W. J. ten Tusscher and A. V. Panfilov

Am J Physiol Heart Circ Physiol 291:H1088-H1100, 2006. First published 24 March 2006;
doi: 10.1152/ajpheart.00109.2006

Also open the paper
"Alternans and Spiral Breakup In a Human Ventricular Tissue Model"

Table 1. *Default model parameter settings*

Parameter	Definition	Value
R	Gas constant	8.3143 J·K^{-1}·mol^{-1}
T	Temperature	310 K
F	Faraday constant	96.4867 C/mmol
C_m	Cell capacitance per unit surface area	2.0 μF/cm^2
S	Surface to volume ratio	0.2 μm^{-1}
ρ	Cellular resistivity	162 Ω-cm
V_c	Cytoplasmic volume	16.404 μm^3
V_{sr}	Sarcoplasmic reticulum volume	1.094 μm^3
V_{ss}	Subspace volume	0.05468 μm^3
K_o	Extracellular K^+ concentration	5.4 mM
Na_o	Extracellular Na^+ concentration	140 mM
Ca_o	Extracellular Ca^{2+} concentration	2 mM
G_{Na}	Maximal I_{Na} conductance	14.838 nS/pF
G_{K1}	Maximal I_{K1} conductance	5.405 nS/pF
G_{to}, epi, M	Epicardial I_{to} conductance	0.294 nS/pF
G_{to}, endo	Maximal endocardial I_{to} conductance	0.073 nS/pF
G_{Kr}	Maximal I_{Kr} conductance	0.153 nS/pF
G_{Ks}, epi, endo	Maximal epi-and endocardial I_{Ks} conductance	0.392 nS/pF
G_{Ks}, M	Maximal M cell I_{Ks} conductance	0.098 nS/pF
p_{KNa}	Relative I_{Ks} permeability to Na^+	0.03
G_{CaL}	Maximal I_{CaL} conductance	3.980^{-5} cm·ms^{-1}·μF^{-1}
k_{NaCa}	Maximal I_{NaCa}	1,000 pA/pF
γ	Voltage dependence parameter of I_{NaCa}	0.35
K_{mCa}	Ca_i half-saturation constant for I_{NaCa}	1.38 mM
K_{mNa}	Na_i half-saturation constant for I_{NaCa}	87.5 mM
k_{sat}	Saturation factor for I_{NaCa}	0.1
α	Factor enhancing outward nature of I_{NaCa}	2.5
P_{NaK}	Maximal I_{NaK}	2.724 pA/pF
K_{mK}	K_o half-saturation constant of I_{NaK}	1 mM
K_{mNa}	Na_i half-saturation constant of I_{NaK}	40 mM
G_{pK}	Maximal I_{pK} conductance	0.0146 nS/pF
G_{pCa}	Maximal I_{pCa} conductance	0.1238 nS/pF
K_{pCa}	Half-saturation constant of I_{pCa}	0.0005 mM
G_{bNa}	Maximal I_{bNa} conductance	0.000290 nS/pF
G_{bCa}	Maximal I_{bCa} conductance	0.000592 nS/pF
V_{maxup}	Maximal I_{up} conductance	0.006375 mM/ms
K_{up}	Half-saturation constant of I_{up}	0.00025 mM
V_{rel}	Maximal I_{rel} conductance	40.8 mM/ms
k_1'	R to O and RI to I I_{rel} transition rate	0.15 mM^{-2}·ms^{-1}
k_2'	O to I and R to RI I_{rel} transition rate	0.045 mM^{-1}·ms^{-1}
k_3	O to R and I to RI I_{rel} transition rate	0.060 ms^{-1}
k_4	I to O and RI to I I_{rel} transition rate	0.000015 ms^{-1}
EC	Ca_{SR} half-saturation constant of k_{casr}	1.5 mM
max_{sr}	Maximum value of k_{casr}	2.5 (dimensionless)
min_{sr}	Minimum value of k_{casr}	1 (dimensionless)
V_{leak}	Maximal I_{Stca} conductance	0.00036 mM/ms
V_{xfer}	Maximal I_{Xfer} conductance	0.0038 mM/ms
Buf_c	Total cytoplasmic buffer concentration	0.2 mM
K_{bufc}	Ca_i half-saturation constant for cytoplasmic buffer	0.001 mM
Buf_{sr}	Total sarcoplasmic buffer concentration	10 mM
K_{bufsr}	Ca_{SR} half-saturation constant for sarcoplasmic buffer	0.3 mM
Buf_{ss}	Total subspace buffer concentration	0.4 mM
K_{bufss}	Ca_{ss} half-saturation constant for subspace buffer	0.00025 mM

I_{Na}, Na^+ current; I_{K1}, inward rectifier K^+ current; I_{to}, transient outward current, I_{Kr}, rapid delayed rectifier current; I_{Ks}, slow delayed rectifier current; I_{CaL}, L-type Ca^{2+} current; I_{NaCa}, Na^+/Ca^{2+} exchanger current; I_{NaK}, Na^+-K^+ pump current; I_{bNa}, background Na^+ current; I_{bCa}, background Ca^{2+} current; I_{pK}, plateau K^+ current; I_{pCa}, sarcolemmal Ca^{2+} pump current; I_{rel}, calcium-induced calcium release current; I_{up}, sarcoplasmic reticulum (SR) Ca^{2+} pump current; I_{leak}, SR Ca^{2+} leak current; I_{Xfer}, diffusive Ca^{2+} current between diadic subspace and bulk cytoplasm; O, open conducting state of I_{rel}; R, resting closed state of I_{rel}; I, inactivated closed state of I_{rel}; RI, resting inactivated closed state of I_{rel}.

Under Numerical Methods
on page 4 (in PDF form)

APPENDIX

No changes were made to formulations of the following currents: I_{Na}, I_{to}, I_{Kr}, I_{K1}, I_{NaCa}, I_{NaK}, I_{pCa}, I_{pK}, I_{bNa}, and I_{bCa}. For these formulations, we refer to their description in the previous version of our model (61).

L-Type Ca^{2+} Current

$$I_{CaL} = G_{CaL} dff_2 f_{cass} 4 \frac{(V-15)F^2}{RT} \frac{0.25Ca_{SS}e^{2(V-15)F/RT} - Ca_o}{e^{2(V-15)F/RT} - 1} \quad (6)$$

$$d_\infty = \frac{1}{1 + e^{(-8-V)/7.5}} \quad (7)$$

Under Appendix
on page 12 (in PDF form)

APPENDIX

No changes were made to formulations of the following currents: I_{Na}, I_{to}, I_{Kr}, I_{K1}, I_{NaCa}, I_{NaK}, I_{pCa}, I_{pK}, I_{bNa}, and I_{bCa}. For these formulations, we refer to their description in the previous version of our model (61).

L-Type Ca^{2+} Current

$$I_{CaL} = G_{CaL}\,dff_2 f_{cass} 4\,\frac{(V-15)F^2}{RT}\,\frac{0.25Ca_{SS}e^{2(V-15)F/RT} - Ca_o}{e^{2(V-15)F/RT} - 1} \qquad (6)$$

$$d_\infty = \frac{1}{1 + e^{(-8-V)/7.5}} \qquad (7)$$

Under Appendix
on page 12 (in PDF form)

$$\alpha_d = \frac{1.4}{1 + e^{(-35-V)/13}} + 0.25 \quad (8)$$

$$\beta_d = \frac{1.4}{1 + e^{(V+5)/5}} \quad (9)$$

$$\gamma_d = \frac{1}{1 + e^{(50-V)/20}} \quad (10)$$

$$\tau_d = \alpha_d \beta_d + \gamma_d \quad (11)$$

$$f_\infty = \frac{1}{1 + e^{(V+20)/7}} \quad (12)$$

$$\alpha_f = 1102.5 e^{-\left(\frac{V+27}{15}\right)^2} \quad (13)$$

$$\beta_f = \frac{200}{1 + e^{(13-V)/10}} \quad (14)$$

$$\gamma_f = \frac{180}{1 + e^{(V+30)/10}} + 20 \quad (15)$$

$$\tau_f = \alpha_f + \beta_f + \gamma_f \quad (16)$$

$$f_2\infty = \frac{0.67}{1 + e^{(V+35)/7}} + 0.33 \quad (17)$$

$$\alpha_{f2} = 600 e^{-\frac{(V+25)^2}{170}} \quad (18)$$

$$\beta_{f2} = \frac{31}{1 + e^{(25-V)/10}} \quad (19)$$

$$\gamma_{f2} = \frac{16}{1 + e^{(V+30)/10}} \quad (20)$$

$$\tau_{f2} = \alpha_{f2} + \beta_{f2} + \gamma_{f2} \quad (21)$$

$$f_{cass\infty} = \frac{0.6}{1 + \left(\frac{Ca_{SS}}{0.05}\right)^2} + 0.4 \quad (22)$$

$$\tau_{fcass} = \frac{80}{1 + \left(\frac{Ca_{SS}}{0.05}\right)^2} + 2 \quad (23)$$

Slow Delayed Rectifier Current

$$I_{Ks} = G_{Ks} x_s^2 (V - E_{Ks}) \quad (24)$$

$$x_{s\infty} = \frac{1}{1 + e^{(-5-V)/14}} \quad (25)$$

$$\alpha_{xs} = \frac{1400}{\sqrt{1 + e^{(5-V)/6}}} \quad (26)$$

$$\beta_{xs} = \frac{1}{1 + e^{(V-35)/15}} \quad (27)$$

$$\tau_{xs} = \alpha_{xs} \beta_{xs} + 80 \quad (28)$$

cytoplasm; O is proportion of open I_{rel} channels; and $\bar{R}$ is proportion of closed I_{rel} channels (for parameters, see Table 1).

$$I_{leak} = V_{leak}(Ca_{SR} - Ca_i) \quad (29)$$

$$I_{up} = \frac{V_{maxup}}{1 + K_{up}^2 / Ca_i^2} \quad (30)$$

$$I_{rel} = V_{rel} O (Ca_{SR} - Ca_{SS}) \quad (31)$$

$$I_{xfer} = V_{xfer}(Ca_{SS} - Ca_i) \quad (32)$$

$$O = \frac{k_1 Ca_{SS}^2 \bar{R}}{k_3 + k_1 Ca_{SS}^2} \quad (33)$$

$$\frac{d\bar{R}}{dt} = -k_2 Ca_{SS} \bar{R} + k_4 (1 - \bar{R}) \quad (34)$$

$$k_1 = \frac{k_{1'}}{k_{casr}} \quad (35)$$

$$k_2 = k_2 k_{casr} \quad (36)$$

$$k_{casr} = max_{sr} - \frac{max_{sr} - min_{sr}}{1 + (EC/Ca_{SR})^2} \quad (37)$$

$$Ca_{ibufc} = \frac{dCa_i \times Buf_c}{dCa_i + K_{bufc}} \quad (38)$$

$$dCa_{itotal}/dt = -\frac{I_{bCa} + I_{pCa} - 2I_{NaCa}}{2V_c F} + \frac{V_{sr}}{V_c}(I_{leak} - I_{up}) + I_{xfer} \quad (39)$$

$$Ca_{srbufsr} = \frac{Ca_{sr} \times Buf_{sr}}{Ca_{sr} + K_{bufsr}} \quad (40)$$

$$dCa_{SRtotal}/dt = (I_{up} - I_{leak} - I_{rel}) \quad (41)$$

$$Ca_{ssbufss} = \frac{Ca_{ss} \times Buf_{ss}}{Ca_{ss} + K_{bufss}} \quad (42)$$

$$dCa_{SStotal}/dt = -\frac{I_{CaL}}{2V_{SS}F} + \frac{V_{sr}}{V_{ss}} I_{rel} - \frac{V_c}{V_{ss}} I_{xfer} \quad (43)$$

```
86
87      data_df.push( 1./(1.+Math.exp((-8.-vv)/7.5)) ); //  dinft
88      var Ad=1.4/(1.+Math.exp((-35.-vv)/13.))+0.25;
89      var Bd=1.4/(1.+Math.exp((vv+5.)/5.));
90      var Cd=1./(1.+Math.exp((50.-vv)/20.));
91      data_df.push( dt/(Ad*Bd+Cd) );                    //  nu_D
92      data_df.push( 1./(1.+Math.exp((vv+20.)/7.)) );  //  finft
93      var Af=1102.5*Math.exp(-(vv+27.)*(vv+27.)/225.);
94      var Bf=200./(1.+Math.exp((13.-vv)/10.));
95      var Cf=(180./(1.+Math.exp((vv+30.)/10.)))+20.;
96      data_df.push( dt/(Af+Bf+Cf) );                    //  nu_F
97      data_fx.push( 0.67/(1.+Math.exp((vv+35.)/7.))+0.33 );  // f2inft
98      var Af2=562.*Math.exp(-(vv+27.)*(vv+27.)/240.);
99      var Bf2=31./(1.+Math.exp((25.-vv)/10.));
100     var Cf2=16./(1.+Math.exp((vv+30.)/10.));
101     data_fx.push( dt/(Af2+Bf2+Cf2) );                 //  nu_F2
102     data_fx.push( 1./(1.+Math.exp((-5.-vv)/14.)) ); // xsinft
103     var Axs=(1400./(Math.sqrt(1.+Math.exp((5.-vv)/6.))));
104     var Bxs=(1./(1.+Math.exp((vv-35.)/15.)));
105     data_fx.push( dt/(Axs*Bxs+80.) );                 // nu_Xs
106
107   var Ko=5.4,Cao=2.0,Nao=140.0,
108       GpK=0.0146,GK1=5.405,alphanaca=2.5,
109       KmK=1.0,KmNa=40.0,
110       knak=2.724,GCaL=0.00003980,
111       knaca=1000,KmNai=87.5,KmCa=1.38,ksat=0.1,
112       n=0.35,
113       KmNai3=KmNai*KmNai*KmNai, Nao3=Nao*Nao*Nao,
114       RR=8314.3,FF=96486.7,TT=310.0,
115       rtof=(RR*TT)/FF, fort=1./rtof;
116
117     var temp=Math.exp(2*(vv-15.001)*fort)
118     data_iCa.push( GCaL*4.*(vv-15.001)*(FF*fort)*(0.25*temp)/(temp-1.) ); // ical1t   ///
119     data_iCa.push( GCaL*4.*(vv-15.001)*(FF*fort)*Cao/(temp-1.) );         // ical2t
120     temp=Math.exp((n-1.)*vv*fort);
121     var temp2=knaca/((KmNai3+Nao3)*(KmCa+Cao)*(1.+ksat*temp));
```

What do we notice here that can be matches in the paper(s) ?

Let's make code/implementations of our own equations, which are based on the paper(s) ...

CLB.CharlesB@gmail.com

Let's make notes & observations about the code and how it relates to the equations ...

Compare the code you created and the code in the draw and tau functions as well as parameters and variables ....

CLB.CharlesB@gmail.com

Thats it ....

Thank You